



# Hybrid Approach Control of Micro-Positioning Stage with a Piezoelectric Actuator

Ounissi Amor<sup>1\*</sup>, Azeddine Kaddouri<sup>2</sup>, Rachid Abdessemed<sup>1</sup>

<sup>1</sup> Department of Electrical Engineering, University of BATNA-2-, 05000 Batna, Algeria

<sup>2</sup> Department of Electrical Engineering, University of Moncton, E1 A3E9 Moncton, NB, Canada

\* Correspondence: Ounissi Amor (amor.ounissi@univ-batna2.dz)

Received: 06-28-2022

Revised: 07-26-2022

Accepted: 08-13-2022

**Citation:** O. Amor, A. Kaddouri, and R. Abdessemed, "Hybrid approach control of micro-positioning stage with a piezoelectric actuator," *J. Intelli Syst. Control*, vol. 1, no. 1, pp. 35-45, 2022. <https://doi.org/10.56578/jisc010104>.



© 2022 by the authors. Licensee Acadlore Publishing Services Limited, Hong Kong. This article can be downloaded for free, and reused and quoted with a citation of the original published version, under the CC BY 4.0 license.

**Abstract:** For a class of system with nonlinear hysteresis, this paper presents an adaptive hybrid controller based on the hybrid backstepping-sliding mode, and describes the controller analytically by the LuGre model. Both backstepping and the sliding mode techniques are based on the Lyapunov theory. Drawing on this common point, the authors developed a new controller combining the two control techniques with a recursive design. The design aims to achieve two effects: assuring the stability of the closed loop system, and improving the continuous performance of the tracking position trajectory. The performance of the proposed hybrid controller was verified by implementing the identified Piezo model. The results show that our controller can track the system output desirably with the reference trajectory.

**Keywords:** Hybrid controller; Particle Swarm Optimization (PSO); LuGre model; Piezo-positioning mechanism

## 1. Introduction

Precision positioning applications increasingly rely on actuation technologies built on intelligent piezoelectric materials. They need compact devices or a small footprint for particular operations [1-4]. Their high integrative power [5, 6], low heat [7, 8], and low noise levels [9, 10] can provide relatively large efforts, high reliability, and biocompatibility [11-14]. Because of these benefits, the piezoelectric actuator has been widely used in a variety of industries, including space exploration [15, 16], active shutters, pulsed jets [17-19], vibration control [20-24], optical path control [25-28], micro-motorization of instruments [29, 30], valves and pumps for implants [31-36], magnetic resonance imaging (MRI) [37, 38], microsurgery [39-42], and other micro-displacement techniques [43-48]. Position control is severely hindered by the unique piezoelectric actuator structure, nonlinear hysteresis behaviors, and additional sources of positioning precision loss, such as creep drift and temperature effects [49-53]. Extensive study has been done for the modeling and control of the nonlinearity of hysteresis. Insofar as it enables the acquisition of a system representation from the input/output data, experimental modeling leading to a model of representation is particularly intriguing [54-58].

This work proposes the LuGre model, which represents the effects of the hysteresis of the piezoelectric actuator with precision and efficiency, and then identifies the control parameters experimentally by the evolutionary algorithm called particle swarm optimization (PSO) [59-65]. The control of piezoelectric actuators has received a lot of attention in recent years. A powerful method for stabilizing nonlinear systems and monitoring trajectory is called backstepping control. The basic goal of backstepping is to achieve Lyapunov cascade stability in equivalent loops in a subsystem of order one, which endows them with robustness and asymptotic overall stability [66-71]. Another very well-known control method is sliding mode control, which is noted for its stability, short response times, and sensitivity to parameter fluctuations [72-76].

A current focus of research is the integration of sliding mode and backstepping control methods within the piezoelectric actuator. In this work, adaptive back stepping-sliding mode, one of the hybrid controls, is employed to enhance the piezoelectric actuator's trajectory tracking capability. The hybrid control technique is a controller design approach that ensures the stability of the control system. The combination between the two control methods

is anticipated to result in a novel control algorithm that takes advantage of the strengths of the two methods. Simulation results demonstrate the strategy's advantage in terms of lowering tracking error and improving tracking stability. The hybrid control exhibits great performance, compared to sliding mode, and adaptive backstepping.

## 2. Stage Modeling and Identification

The dynamic model of the piezoelectric actuator can be expressed as [77]:

$$M\ddot{x} + D\dot{x} + F_H + F_L = k_e u \quad (1)$$

where,  $M$  is the equivalent mass of the piezoelectric actuator;  $x$  is the displacement of the mechanism;  $\dot{x}$  is the relative velocity;  $\ddot{x}$  is the acceleration;  $D$  is the linear friction coefficient of the piezoelectric actuator;  $F_L$  is the external load;  $F_H$  is the function of the hysteresis friction force;  $u$  is the voltage applied to the piezoelectric actuator. The hysteresis friction force  $F_H$  can be described by LuGre model [78]:

$$F_H = \sigma_0 \cdot x_2 - \sigma_1 \frac{1}{g(x_2)} x_2 |x_2| + (\sigma_1 + \sigma_2) x_2 \quad (2)$$

where,  $\sigma_0$ ,  $\sigma_1$ , and  $\sigma_2$  are positive constants, which can be equivalently interpreted as the bristle stiffness, bristle damping and viscous coefficient, respectively. The Stribeck effect curve can be described by the function  $g(x_2)$ :

$$\sigma_0 \cdot g(x_2) = f_c + (f_s - f_c) e^{-(x_2/x_s)^2} \quad (3)$$

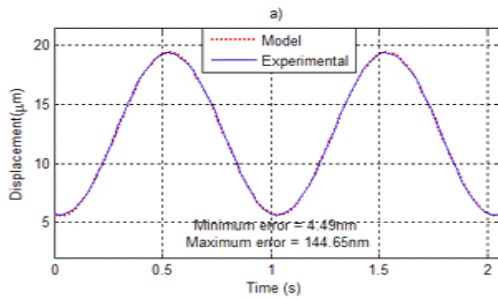
where,  $f_c$  is the Coulomb friction;  $f_s$  is the striction force;  $x_s$  is the Stribeck velocity. The complete electromechanical equations for the model can be expressed as [79]:

$$\dot{x}_2 = \frac{k_e u}{M} - \frac{\sigma_0 \cdot x_2}{M} - \frac{\sigma_1}{M} \frac{1}{g(x_2)} x_2 |x_2| + \frac{(\sigma_1 + \sigma_2)}{M} x_2 + \frac{F_L}{M} - \frac{Dx_1}{M} \quad (4)$$

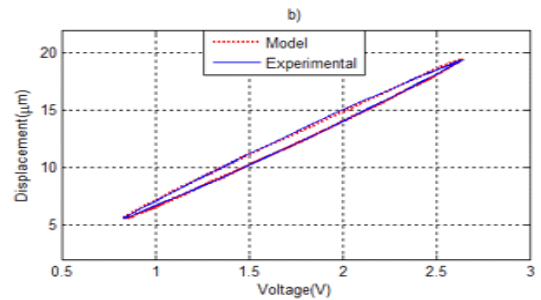
Eq. (4) shows that the piezoelectric actuator's dynamics is nonlinear as a function of the state variables  $x_1$  and  $x_2$ , and that the relationship between position and control voltage must be monitored in order to obtain the parameters of the LuGre model. This paper utilizes the PSO-based identification approach, and runs tests to optimize the parameters of the algorithm and the model. Table 1 displays the values for the nine parameters.

**Table 1.** Identification results for the LuGre model

Parameter	Value	Unit
$M$	4.119	g
$k_e$	93.6	N/v
$\sigma_0$	$2.176e^{+06}$	N/m
$\sigma_1$	$4.257e^{+06}$	N <sub>s</sub> /m
$\sigma_2$	$-3.826e^{+06}$	N <sub>s</sub> /m
$F_c$	6224	N
$F_s$	$-7.181e^{+04}$	N <sub>s</sub> /m
$x_s$	0.7621	m/s
$D$	10.76	N <sub>s</sub> /m



(a) Sinusoidal signal



(b) Linear signal

**Figure 1.** Tracking performance with LuGre model

Figure 1 compares the tracking performance of LuGre model with that of experiments, when the piezoelectric positioning stage is driven by a sinusoidal input or a linear input. The comparison shows that the minimum and maximum errors are 4.492 nm and 144.65 nm, respectively. The experimental results agree well with the LuGre modeling results.

## 2.1 Hybrid Control

The control law can be generated according to two sequences. The first sequence adopts the backstepping technique to compute the virtual controls and the corresponding stabilization functions.

### 2.1.1 First sequence

The nonlinear system can be described by:

$$\begin{aligned}\dot{x}_1 &= \Psi_1(x_1) \cdot x_2 + \varphi_1(x_1)^T \cdot \theta \\ \dot{x}_2 &= \Psi_2(x_1, x_2) \cdot x_3 + \varphi_2(x_1, x_2)^T \cdot \theta \\ \dot{x}_{n-1} &= \Psi_{n-1}(x_1, \dots, x_{n-1}) \cdot x_n + \varphi_{n-1}(x_1, \dots, x_{n-1})^T \cdot \theta \\ \dot{x}_n &= \Psi_{n-1}(x_1, \dots, x_{n-1}, \dots, x_n) \cdot u + \varphi_{n-1}(x_1, \dots, x_{n-1}, \dots, x_n)^T \cdot \theta\end{aligned}\quad (5)$$

where,  $\varphi_i: R^i \rightarrow R^p$  is a continuously differentiable vector of known nonlinear functions;  $\theta \in R^p$  - a vector of constant coefficients (known or unknown);  $\Psi_{n-1}$  is a function  $\neq 0 \forall x \in R^n$  u the control. To track the desired trajectory  $x_d$  using the state  $x_i$ , then the backstepping algorithm can be used for the overall asymptotic stabilization of the system error  $e \in R^n$ . To better illustrate this technique, the second-order nonlinear system can be considered in the following form:

$$\begin{aligned}\dot{x}_1 &= x_2 + \varphi_1(x_1)^T \cdot \theta \\ \dot{x}_2 &= u + \varphi_2(x_1, x_2)^T \cdot \theta\end{aligned}\quad (6)$$

With  $x=[x_1, x_2]$ , the state vector and system control input  $u(t)$ , the problem is to determine the control  $u(t)$  that stabilizes the system at point  $(x_1, x_2) = (0,0)$  [80].

To achieve the desired trajectory and stabilize the entire system, it is preferable to use an adaptive law to estimate the system parameters by the backstepping technique. Suppose the output variable is denoted by  $x_1$  and the certain desired trajectory is denoted by  $x_{1d}$ , the quantity of the control can be selected in two steps:

### A.1 First step

This first step consists in identifying the error and it is dynamic

$$e_1 = x_1 - x_d$$

The derivative of the error can be expressed as:

$$\begin{aligned}\dot{e}_1 &= \dot{x}_1 - \dot{x}_d = e_2 - \alpha_1 \\ &\text{where,} \\ \alpha_1 &= -c_1 e_1 \\ \dot{e}_1 &= -c_1 e_1 + e_2\end{aligned}\quad (7)$$

Considering the Lyapunov function:

$$V_1 = \frac{1}{2} e_1^2 \quad (8)$$

The derivative can be obtained as:

$$\begin{aligned}\dot{V}_1 &= e_1 \dot{e}_1 \\ &= e_1 (-c_1 e_1 + e_2) \\ &= -c_1 e_1^2 + e_1 e_2\end{aligned}\quad (9)$$

From Eq. (9), it is known that if  $e_2(t)$  tends to zero, the derivative of  $V_1(t)$  will be less than or equal to zero. If  $V_1 \leq 0$ ,  $e_1(t)$  will converge to zero, and  $x_1(t)$  will converge to the reference point  $x_d$ . Consequently, the next step will design a controller  $u$  to make  $e_2(t)$  converge towards zero.

## A.2 Second step

Considering the second system error:  $e_2 = x_2 - \alpha_1 - \dot{x}_d$

$$\begin{aligned} e_2 &= x_2 - \alpha_1 - \dot{x}_d \\ \text{With} \\ \dot{e}_2 &= \dot{x}_2 - \dot{\alpha}_1 - \ddot{x}_d \\ &= \frac{1}{k_0} u - k_1 x_2 - k_2 x_1 - h(t) - \dot{\alpha}_1 - \ddot{x}_d \\ u &= \hat{k}_0 \bar{u} - \hat{k}_3 \text{sign}(e_2) \end{aligned} \quad (10)$$

Alternatively,  $\hat{k}_0, \hat{k}_1, \hat{k}_2$ , and  $\hat{k}_3$  are the estimated values of  $k_0, k_1, k_2$ , and  $k_3$ ,  $\tilde{k}_0 = \hat{k}_0 - k_0, \tilde{k}_1 = \hat{k}_1 - k_1, \tilde{k}_2 = \hat{k}_2 - k_2$ , and  $\tilde{k}_3 = \hat{k}_3 - k_3$ , respectively;  $\text{sign}(\cdot)$  denotes the sign function:

$$\text{sign}(e_2) = \begin{cases} 1 & \text{if } e_2 > 0 \\ 0 & \text{if } e_2 = 0 \\ -1 & \text{if } e_2 < 0 \end{cases} \quad (11)$$

The Lyapunov function  $V_2$  can be defined as:

$$V_2 = \frac{1}{2} e_1^2 + \frac{1}{2} e_2^2 + \frac{1}{2k_0\alpha_0} \tilde{k}_0^2 + \frac{1}{2\alpha_1} \tilde{k}_1^2 + \frac{1}{2\alpha_2} \tilde{k}_2^2 + \frac{1}{2\alpha_3} \tilde{k}_3^2 \quad (12)$$

The derivative can be obtained by:

$$\dot{V}_2 = e_1 \dot{e}_1 + e_2 \dot{e}_2 + \frac{1}{k_0\alpha_0} \tilde{k}_0 \dot{\tilde{k}}_0 + \frac{1}{\alpha_1} \tilde{k}_1 \dot{\tilde{k}}_1 + \frac{1}{\alpha_2} \tilde{k}_2 \dot{\tilde{k}}_2 + \frac{1}{\alpha_3} \tilde{k}_3 \dot{\tilde{k}}_3 \quad (13)$$

$$\begin{aligned} \dot{V}_2 &= c_1 e_1^2 + e_1 e_2 + e_2 \left( \frac{1}{k_0} u - k_1 x_2 - k_2 x_1 - k_3 - \dot{\alpha}_1 \right) + \frac{1}{k_0\alpha_0} \tilde{k}_0 \dot{\tilde{k}}_0 + \frac{1}{\alpha_1} \tilde{k}_1 \dot{\tilde{k}}_1 + \frac{1}{\alpha_2} \tilde{k}_2 \dot{\tilde{k}}_2 \\ &\quad + \frac{1}{M\alpha_3} \tilde{k}_3 \dot{\tilde{k}}_3 \end{aligned} \quad (14)$$

With

$$\frac{1}{k_0} u = \bar{u} - \frac{1}{k_0} \hat{k}_0 \bar{u} - \hat{k}_3 \text{sign}(e_2) \quad (15)$$

$$\begin{aligned} \dot{V}_2 &= c_1 e_1^2 + e_1 e_2 + e_2 (\bar{u} + e_1 - k_1 x_2 - k_2 x_1 - \dot{\alpha}_1 - \ddot{x}_{1d}) - (k_3 - \hat{k}_3 \text{sign}(e_2)) + \frac{1}{k_0\alpha_0} \tilde{k}_0 \dot{\tilde{k}}_0 \\ &\quad + \frac{1}{\alpha_1} \tilde{k}_1 \dot{\tilde{k}}_1 + \frac{1}{\alpha_2} \tilde{k}_2 \dot{\tilde{k}}_2 + \frac{1}{\alpha_3} \tilde{k}_3 \dot{\tilde{k}}_3 \\ &= c_1 e_1^2 + e_1 e_2 + e_2 (\bar{u} + e_1 - k_1 x_2 - k_2 x_1 - \dot{\alpha}_1 - \ddot{x}_{1d}) - (k_3 - \hat{k}_3 \text{sign}(e_2)) \\ &\quad + \frac{1}{k_0\alpha_0} \tilde{k}_0 (\alpha_0 e_2 \bar{u} + \dot{\tilde{k}}_0) + \frac{1}{\alpha_1} \tilde{k}_1 (\alpha_1 x_1 e_2 + \dot{\tilde{k}}_1) + \frac{1}{\alpha_2} \tilde{k}_2 (\alpha_2 x_2 e_2 + \dot{\tilde{k}}_2) \\ &\quad + \frac{1}{\alpha_3} \tilde{k}_3 (\alpha_3 |e_2| - \dot{\tilde{k}}_3) - e_2 \bar{u} \hat{k}_0 - e_2 x_2 \hat{k}_1 - e_2 x_1 \hat{k}_2 - |e_2| \hat{k}_3 x_2 \end{aligned} \quad (16)$$

$c_1$  and  $c_2$  are positive defined constants. Then, the control law can be selected as:

$$\bar{u} = -c_2 e_2 - e_1 - e_2 \bar{u} \hat{k}_0 - e_2 x_2 \hat{k}_1 - e_2 x_1 \hat{k}_2 - |e_2| \hat{k}_3 x_2 - \eta \cdot \text{sign}(e_2) - \ddot{x}_{1d} \quad (17)$$

With the following adaptation laws:

$$\dot{\hat{k}}_0 = -\alpha_0 e_2 \bar{u} \quad (18)$$

$$\dot{\hat{k}}_1 = \alpha_1 e_2 x_2 \quad (19)$$

$$\dot{\hat{k}}_2 = \alpha_1 e_2 x_1 \quad (20)$$

$$\dot{\hat{k}}_3 = \alpha_3 e_2 \quad (21)$$

Substituting the adaptation laws (17), (18), (19), and (20) into Eq. (16), we have:

$$\dot{V}_2 = -c_1 e_1^2 - c_2 e_2^2 \quad (22)$$

This means the equilibrium of the closed-loop system is globally asymptotically stable, and the error variables  $e_1$  and  $e_2$  converge towards zero.

## B. Second sequence

The second sequence highlights the sliding mode technique to calculate the real controls in the final backstepping step. The goal is to make the errors between the virtual controls and their desired values converge to zero. The introduction of the sliding control reduces the effects of disturbances. The hybridization between the backstepping control and the sliding mode control is realized by changing a variable in the last step [81].

To being with, the linear sliding surface can be considered as:

$$S = \lambda_1 e_1 + \dot{e}_1 \quad (23)$$

With  $\lambda_1 > 0$ , the derivative of Eq. (23) can be obtained as:

$$\dot{S} = \lambda_1 e_2 + \dot{e}_2 \quad (24)$$

Therefore, the modified Lyapunov candidate can be expressed as:

$$V_2 = \frac{1}{2} e_1^2 + \frac{1}{2} e_2^2 + \frac{1}{2k_0\alpha_0} \tilde{k}_0^2 + \frac{1}{2\alpha_1} \tilde{k}_1^2 + \frac{1}{2\alpha_2} \tilde{k}_2^2 + \frac{1}{2\alpha_3} \tilde{k}_3^2 + \frac{1}{2} S^2 \quad (25)$$

Then, the derivative of  $V_2$  can be given by:

$$\begin{aligned} \dot{V}_2 = & -c_1 e_1^2 + e_1 e_2 + e_2 (\dot{e}_2) + \frac{1}{k_0\alpha_0} \tilde{k}_0 (\alpha_0 e_2 \bar{u} + \dot{\tilde{k}}_0) + \frac{1}{\alpha_1} \tilde{k}_1 (\alpha_1 x_1 e_2 + \dot{\tilde{k}}_1) + \frac{1}{\alpha_2} \tilde{k}_2 (\alpha_2 x_2 e_2 + \dot{\tilde{k}}_2) \\ & + \frac{1}{\alpha_3} \tilde{k}_3 (\alpha_3 |e_2| - \dot{\tilde{k}}_3) - e_2 \bar{u} \tilde{k}_0 - e_2 x_2 \hat{k}_1 - e_2 x_1 \hat{k}_2 - |e_2| + S(\lambda_1 e_2 + \dot{e}_2) \end{aligned} \quad (26)$$

Substituting Eq. (10) into Eq. (25), we have:

$$\begin{aligned} \dot{V}_2 = & -c_1 e_1^2 + e_1 e_2 + e_2 (\bar{u} + e_1 - k_1 x_2 - k_2 x_1 - \dot{\alpha}_1 - \ddot{x}_{1d}) - (k_3 - \hat{k}_3 \text{sign}(e_2)) \\ & + \frac{1}{k_0\alpha_0} \tilde{k}_0 (\alpha_0 (e_2 + S) \bar{u} + \dot{\tilde{k}}_0) + \frac{1}{\alpha_1} \tilde{k}_1 (\alpha_1 x_1 (e_2 + S) + \dot{\tilde{k}}_1) \\ & + \frac{1}{\alpha_2} \tilde{k}_2 (\alpha_2 x_2 (e_2 + S) + \dot{\tilde{k}}_2) + \frac{1}{\alpha_3} \tilde{k}_3 (\alpha_3 (|e_2| + S) - \dot{\tilde{k}}_3) - (e_2 + S) \bar{u} \tilde{k}_0 \\ & - (e_2 + S) x_2 \hat{k}_1 - (e_2 + S) x_1 \hat{k}_2 - (|e_2| + S) \end{aligned} \quad (27)$$

From Eq. (16), the hybrid control law of the piezoelectric actuator can be expressed as:

$$\frac{1}{k_0} u = \bar{u} \left( 1 - \frac{1}{k_0} \hat{k}_0 \right) - \hat{k}_3 \text{sign}(e_2 + S) \quad (28)$$

Thus,

$$\begin{aligned} \bar{u} = & -c_2 e_2 - e_1 - (e_2 + S) \bar{u} \tilde{k}_0 - (e_2 + S) x_2 \hat{k}_1 - (e_2 + S) x_1 \hat{k}_2 - (|e_2| + S) \hat{k}_3 x_2 - \eta \cdot \text{sign}(e_2 + S) \\ & - \ddot{x}_{1d} - \lambda_1 e_2 S \end{aligned} \quad (29)$$

With the adaptation laws

$$\dot{\hat{k}}_0 = -\alpha_0 \bar{u} (S + e_2) \quad (30)$$

$$\dot{\hat{k}}_1 = \alpha_1 x_2 (S + e_2) \quad (31)$$

$$\dot{\hat{k}}_2 = \alpha_1 x_1 (S + e_2) \quad (32)$$

$$\dot{\hat{k}}_3 = \alpha_3 (S + e_2) \quad (33)$$

The control law (29), and the adaptation laws in Eqns. (30-33) can be replaced to obtain:

$$\dot{V}_2 = -c_1 e_1^2 - c_2 e_2^2 \quad (34)$$

The relationship (34) shows that, with the law of hybridization control (28) and the adaptation parameters (30-33), the variables  $e_1(t)$  and  $e_2(t)$  converge towards zero, which allows the exit in pursuit of system (1) following asymptotically the reference.

### 3. Results and Discussion

Figures 2-4 respectively display the tracking displacement, tracking voltage control error, and phase diagram of the simulations on the proposed hysteresis model of piezoelectric positioning mechanism, with an amplitude of the sinusoidal reference of 1  $\mu\text{m}$  and a frequency of 0.5 Hz. It can be seen that the hybrid control managed to stabilize the closed-loop system, and the trajectory tracking effect.

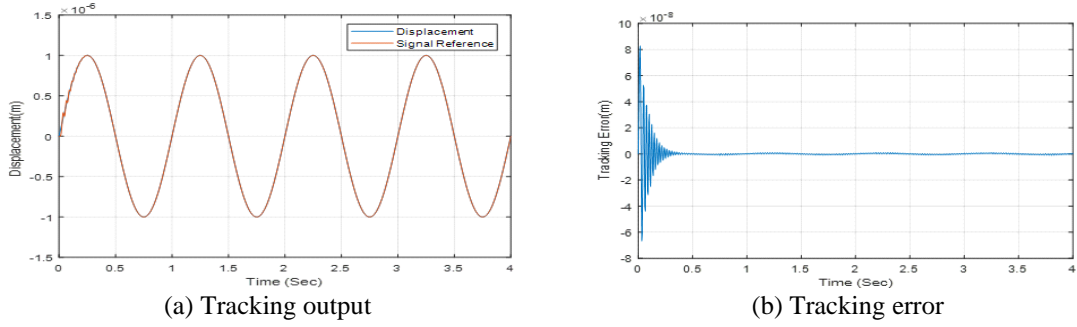


**Figure 2.** Simulation results with a tracking signal of 1.0 Hz

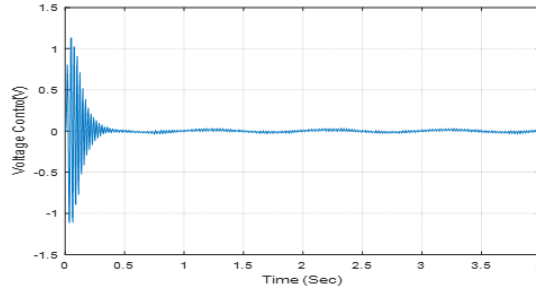


**Figure 3.** Simulation results for periodic sinusoidal control with frequency 1.0 Hz: Voltage control

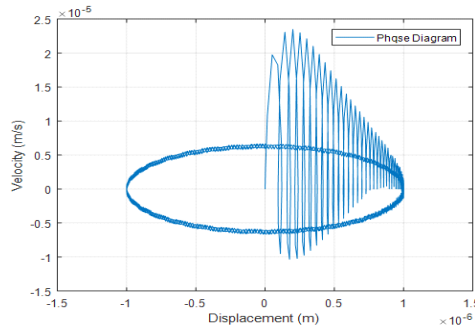


**Figure 4.** Phase diagram

Figure 5 illustrates the convergence of the control parameters ( $k_0$ ,  $k_1$ , and  $k_2$ ). It is clear that the hybrid controller can converge very quickly.

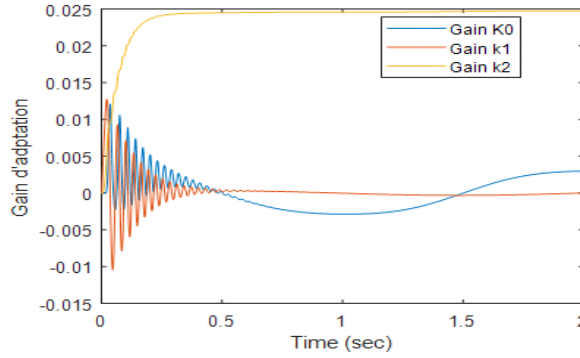


**Figure 5.** Evolution of parameters  $k_0$ ,  $k_1$  and  $k_2$

#### 4. Comparative Analysis

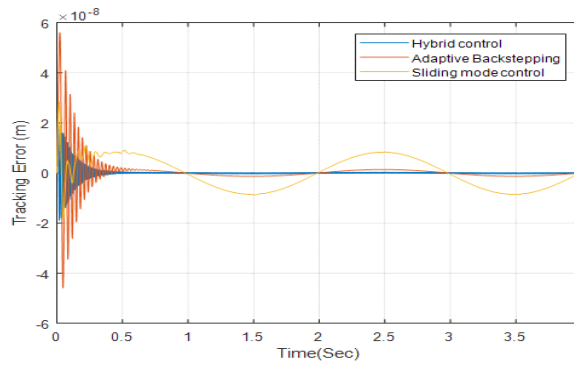
To verify the performance of different control laws for the piezoelectric actuator, a comparative analysis was carried out between the hybrid control, the adaptive backstepping control and the sliding mode control under the same conditions (e.g., the simulation time, the frequency and the input signal). The comparison criterion was defined as a function of the simulation error.

Figure 6 shows how the tracking error of the three techniques evolves. It can be seen that these techniques are valid for the piezoelectric actuator control. The errors suggest that the hybrid controller achieves better results than the adaptive backstepping controller and the sliding mode controller.

Table 2 compares the convergence time for the different control techniques.

**Table 2.** Convergence time of different controllers

Control technique	Convergence time (s)
Hybrid	0.35
Adaptive backstepping	0.6
Sliding mode	0.7



**Figure 6.** Evolution of tracking error for the three control techniques

#### 5. Conclusions

This paper proposes the LuGre model and the associated identification procedure, aiming to accurately depict the hysteresis behavior of the piezoelectric actuator. Besides, a hybrid control was implemented to validate the accuracy of the model. The results show that the proposed method can track the reference trajectory very precisely. The proposed control technique was found to improve the control performance, thanks to its merits like flexible selection of control gains, and the simplicity of forming the control law. In addition, three techniques were compared, including our technique, suggesting that our technique achieves better performance than the contrastive methods.

## Data Availability

The data used to support the findings of this study are available from the corresponding author upon request.

## Conflicts of Interest

The authors declare that they have no conflicts of interest.

## References

- [1] I. Chilibon, "Piezoelectric structures and low power generation devices," *Sensors & Transducers*, vol. 205, no. 10, pp. 16-24, 2016.
- [2] I. Gablech, J. Kelmpa, J. Pekárek, P. Vyroubal, J. Harbina, M. Holá, J. Kunz, J. Brodský, and P. Neuzil, "Simple and efficient AIN-based piezoelectric energy harvesters," *Micromachines*, vol. 11, no. 2, pp. 143-143, 2020. <https://doi.org/10.3390/mi11020143>.
- [3] J. S. Pulskamp, R. G. Polcawich, R. Q. Rudy, S. S. Bedair, R. M. Proie, T. Ivanov, and G. L. Smith, "Piezoelectric PZT MEMS technologies for small-scale robotics and RF applications," *MRS Bull.*, vol. 37, no. 11, pp. 1062-1070, 2012. <https://doi.org/10.1557/mrs.2012.269>.
- [4] M. Pohanka, "Overview of piezoelectric biosensors, immunosensors and DNA sensors and their applications," *Mater.*, vol. 13, no. 3, pp. 448-448, 2018. <https://doi.org/10.3390/ma11030448>.
- [5] A. Zaszczynska, P. Sajkiewicz, and A. Gradys, "Piezoelectric scaffolds as smart materials for neural tissue engineering," *Polym.*, vol. 12, no. 1, pp. 161-161, 2020. <https://doi.org/10.3390/polym12010161>.
- [6] Z. B. Yang, S. X. Zhou, J. Zu, and D. Inman, "High-performance piezoelectric energy harvesters and their applications," *Joule*, vol. 2, no. 4, pp. 642-697, 2018. <https://doi.org/10.1016/j.joule.2018.03.011>.
- [7] Y. K. Yong and A. J. Fleming, "Piezoelectric actuators with integrated high-voltage power electronics," *IEEE/ASME Transac. Mech.*, vol. 20, no. 2, pp. 611-617, 2015. <https://doi.org/10.1109/TMECH.2014.2311040>.
- [8] M. Safaei, H. A. Sodano, and S. R. Anton, "A review of energy harvesting using piezoelectric materials: State-of-the-art a decade later (2008-2018)," *Smart Mater. Struct.*, vol. 28, no. 11, Article ID: 113001, 2019. <https://doi.org/10.1088/1361-665X/ab36e4>.
- [9] N. C. Pisenti, A. Restelli, B. J. Reschovsky, D. S. Barker, and G. K. Campbell, "An ultra-low noise, high-voltage piezo driver," *Rev. Sci Instrum.*, vol. 87, no. 12, Article ID: 124702, 2016. <https://doi.org/10.1063/1.4969059>.
- [10] E. D. Pinheiro and T. Deivarajan, "A concise review encircling lead free porous piezoelectric ceramics," *Acta Phys. Pol. A*, vol. 136, no. 3, pp. 555-565, 2019. <https://doi.org/10.12693/APhysPolA.136.555>.
- [11] L. F. Walubita, D. C. S. Djebou, A. N. M. Faruk, S. I. Lee, S. Dessouky, and X. D. Hu, "Prospective of societal and environmental benefits of piezoelectric technology in road energy harvesting," *Sustain.*, vol. 10, no. 2, pp. 383-383, 2018. <https://doi.org/10.3390/su10020383>.
- [12] S. Trolier-McKinstry, S. J. Zhang, A. J. Bell, and X. L. Tan, "High-performance piezoelectric crystals, ceramics, and films," *Annu Rev. Mater. Res.*, vol. 48, pp. 191-217, 2018. <https://doi.org/10.1146/annurev-matsci-070616-124023>.
- [13] M. T. Todaro, F. Guido, L. Algieri, V. M. Mastronardi, D. Desmaële, G. Epifani, and M. De Vittorio, "Biocompatible, flexible and compliant energy harvesters based on piezoelectric thin films," *IEEE Transac. Nanotechnology*, vol. 17, no. 2, pp. 220-230, 2018. <https://doi.org/10.1109/tnano.2017.2789300>.
- [14] L. Algieri, M. T. Todaro, F. Guido, L. Blasi, V. Mastronardi, D. Desmaële, A. Quattieri, C. Giannini, T. Sibillano, and M. De Vittorio, "Piezoelectricity and biocompatibility of flexible  $\text{Sc}_x\text{Al}_{(1-x)}\text{N}$  thin films for compliant MEMS transducers," *ACS Appl Mater Interfaces*, vol. 12, no. 16, pp. 18660-18666, 2020. <https://doi.org/10.1021/acsami.0c00552>.
- [15] H. Hoshyarmanesh, M. Ghodsi, M. Kim, H. H. Cho, and H. Park, "Temperature effects on electromechanical response of deposited piezoelectric sensors used in structural health monitoring of aerospace structures," *Sensors*, vol. 19, no. 12, pp. 2085-2085, 2019. <https://doi.org/10.3390/s19122805>.
- [16] F. Ksica, Z. Hadas, and J. Hlinka, "Application of piezoelectric sensors for structural health monitoring in aerospace," In 2018 5th IEEE Inter Workshop on Metrology for Aero Space, Rome, Italy, June 20-22, 2018, IEEE, Article ID: 18062376. <https://doi.org/10.1109/MetroAeroSpace.2018.8453610>.
- [17] W. Bowden, I. R. Hill, P. E. G. Baird, and P. Gill, "A high-performance, low-cost laser shutter using a piezoelectric cantilever actuator," *Rev. Sci Instrum.*, vol. 88, no. 1, Article ID: 016102, 2017. <https://doi.org/10.1063/1.4973774>.
- [18] V. Jurenas, R. Bansevicius, and S. Navickaite, "Piezoelectric bimorphs for laser shutter systems: Optimization of dynamic characteristics," *Mechanika*, vol. 5, no. 5, pp. 44-47, 2010.



- [19] K. Li, J. Liu, W. Chen, and L. Zhang, "Effects of pulse voltage on piezoelectric micro-jet for lubrication," *Microsyst Technol.*, vol. 23, pp. 3081-3089, 2016. <https://doi.org/10.1007/s00542-016-3080-3>.
- [20] S. Herold and D. Mayer, "Adaptive piezoelectric absorber for active vibration control," *Actuators*, vol. 5, no. 1, pp. 7-7, 2016. <https://doi.org/10.3390/act5010007>.
- [21] P. A. Thorat, B. C. Londhe, and T. B. Sonawane, "Vibration control by piezoelectric materials: A review," *Inter J. Innov Res. Adv Eng.*, vol. 1, no. 4, pp. 206-210, 2014.
- [22] Z. L. Hu and G. P. Maul, "Vibration control of piezoelectric actuator by implementation of optical positioning sensor," *Int J. Optomechatron.*, vol. 1, no. 4, pp. 369-382, 2007. <https://doi.org/10.1080/15599610701672561>.
- [23] H. Shen, J. H. Qiu, H. L. Ji, K. J. Zhu, M. Balsi, I. Giorgio, and F. Dell'Isola, "A low-power circuit for piezoelectric vibration control by synchronized switching on voltage sources," *Sens. Actuat. A: Phys.*, vol. 161, no. 1-2, pp. 245-255, 2010. <https://doi.org/10.1016/j.sna.2010.04.012>.
- [24] S. O. R. Moheimani and A. J. Fleming, "Piezoelectric transducers for vibration control and damping," In *Series: Advances in Industrial Control*, Springer London, 2006. <https://doi.org/10.1007/1-84628-332-9>.
- [25] E. Magnan, J. Maslek, C. Bracamontes, A. Restelli, T. Boulier, and J. V. Porto, "A low-steering piezo-driven mirror," *Rev. Sci Instrum.*, vol. 89, Article ID: 073110, 2018. <https://doi.org/10.1063/1.5035326>.
- [26] M. J. Mescher, M. L. Vladimer, and J. J. Bernstein, "A novel high - speed piezoelectric deformable varifocal mirror for optical applications," In Technical Digest. MEMS 2002 IEEE International Conference, Fifteenth IEEE International Conference on Micro Electro Mechanical Systems, Las Vegas, NV, USA, January 24-24, 2002. <https://doi.org/10.1109/MEMSYS.2002.984321>.
- [27] V. M. Gelikonov, G. V. Gelikonov, S. Y. Ksenofontov, D. A. Terpelov, and P. A. Shilyagin, "A control system for the optical fiber piezoelectric modulator of the optical path," *Instrum. Exp. Tech+*, vol. 53, no. 3, pp. 443-446, 2010. <https://doi.org/10.1134/S0020441210030218>.
- [28] K. L. Wlodarczyk, E. Bryce, N. Schwartz, M. Strachan, D. Hutson, R. R. J. Maier, D. Atkinson, S. Beard, T. Baillie, P. Parr-Burman, K. Kirk, and D. P. Hand, "Scalable stacked array piezoelectric deformable mirror for astronomy and laser processing applications," *Rev. Sci. Instrum.*, vol. 85, Article ID: 024502, 2014. <https://doi.org/10.1063/1.4865125>.
- [29] M. Kamali, S. A. Jazayeri, F. Najafiv, K. Kawashima, and T. Kagawa, "Study on the performance and control of a piezo-actuated nozzle-flapper valve with an isothermal chamber," *Stroj. Vestn. – J. Mech. E.*, vol. 62, no. 5, pp. 318-328, 2016. <https://doi.org/10.5545/sv-jme.2015.3339>.
- [30] K. Srinivasa Rao, M. Hamza, P. Ashok Kumar, and K. Giriya, "Design and optimization of MEMS based piezoelectric actuator for drug delivery systems," *Microsyst. Technol.*, vol. 26, pp. 1671-1679, 2020. <https://doi.org/10.1007/s00542-019-04712-9>.
- [31] J. Thakkar, P. M. George, N. J. Manek, and P. Chahan, "A valve-less micro pump driven by a piezoelectric actuator," In National Conference on Recent Trends in Engineering & Technology, Vallabh Vidyanagar, Gujarat, India, May 13-14, 2011, Birla Vishvakarma Mahavidyalaya Engineering College, pp. 1-5.
- [32] H. Gensler, R. Sheybani, P. Y. Li, R. Lo, and E. Meng, "An implantable MEMS micropump system for drug delivery in small animals," *Biomed. Microdevices*, vol. 14, no. 3, pp. 483-496, 2012. <https://doi.org/10.1007/s10544-011-9625-4>.
- [33] N. S. Vatkar and Y. S. Vatkar, "Piezoelectric motors & its applications," *Int Res J. Eng. Technol.*, vol. 3, no. 6, pp. 986-990, 2016.
- [34] P. H. Cazorla, O. Fuchs, M. Cochet, and S. Maubert, "Piezoelectric Micro-pump with PZT thin film for low consumption microfluidic devices," *Procedia Engineer.*, vol. 87, pp. 488-491, 2014. <https://doi.org/10.1016/j.proeng.2014.11.402>.
- [35] M. Z. Yıldız and H.A. Dereshgi, "Design and analysis of PZT micropumps for biomedical applications: Glaucoma treatment," *J. Eng. Res.*, vol. 7, no. 2, pp. 202-217, 2019.
- [36] C. Hernandez, Y. Bernard, and A. Razeq, "A global assessment of piezoelectric actuated micro-pumps," *Eur Phys J. Appl Phys.*, vol. 51, no. 2, Article ID: 20101, 2010. <https://doi.org/10.1051/epjap/2010090>.
- [37] N. V. Tsekos, A. Khanicheh, E. Christoforou, and C. Mavroidis, "Magnetic resonance-compatible robotic and mechatronics systems for image-guided interventions and rehabilitation: A review study," *Annu. Rev. Biomed. Eng.*, vol. 9, pp. 351-387, 2007. <https://doi.org/10.1146/annurev.bioeng.9.121806.160642>.
- [38] T. McPherson and J. Ueda, "A force and displacement self-sensing piezoelectric MRI-compatible tweezer end effector with an on site calibration procedure," *IEEE-ASME T. Mech.*, vol. 19, no. 2, pp. 755-764, 2014. <https://doi.org/10.1109/TMECH.2013.2257827>.
- [39] M. Chen-Glasser, P. P. Li, J. Ryu, and S. Hong, "Piezoelectric materials for medical applications," In *Piezoelectricity - Organic and Inorganic Materials and Applications*, London, United Kingdom: IntechOpen, 2018. <https://doi.org/10.5772/intechopen.76963>.
- [40] P. R. Hennet, "Piezoelectric bone surgery: A review of the literature and potential applications in veterinary oromaxillofacial surgery," *Front. Vet. Sci.*, vol. 2, 2015. <https://doi.org/10.3389/fvets.2015.00008>.
- [41] A. Kachroudi, S. Basrou, L. Rufer, and F. Jomni, "Piezoelectric cellular micro-structured PDMS material

- for micro-sensors and energy harvesting,” *J. Phys.: Conf. Ser.*, vol. 660, Article ID: 012040, 2015. <https://doi.org/10.1088/1742-6596/660/1/012040>.
- [42] S. Stübinger, A. Stricker, and B. I. Berg, “Piezosurgery in implant dentistry,” *Clin. Cosmet. Investig. Dent.*, vol. 7, pp. 115-124, 2015. <https://doi.org/10.2147/CCIDE.S63466>.
- [43] S. M. Afonin, “Coded control of Piezoactuator nano - and Microdisplacement for mechatronics systems,” In *Springer Proceedings in Physics*, I. Parinov, S. H. Chang, and V. Gupta, (Eds.), Springer, Cham, vol. 207, pp. 579-584, 2017. [https://doi.org/10.1007/978-3-319-78919-4\\_45](https://doi.org/10.1007/978-3-319-78919-4_45).
- [44] X. D. Chen, S. Y. Hu, Z. L. Deng, J. H. Gao, and X. J. Gao, “Design of large-displacement asymmetric piezoelectric microgripper based on flexible mechanisms,” *Nanotechnol. Precis. Eng.*, vol. 2, no. 4, pp. 188-193, 2019. <https://doi.org/10.1016/j.npe.2019.11.001>.
- [45] T. Takeshita, T. Iwasaki, K. Harisaki, H. Ando, E. Higurashi, and R. Sawada, “Development of a piezo-driven mechanical stage integrated microdisplacement sensor for calibration of displacements,” *Sensor. Mater.*, vol. 26, no. 8, pp. 547-557, 2014.
- [46] P. J. Nandujith, K. G. Vasantha Kumari, S. Sushanth, K. Blesson, M. S. Prasad, and N. Raghu, “Design and fabrication of a piezo actuated flapping mechanism for a micro aerial vehicle,” *J. Aerosp. Eng. Technol.*, vol. 7, no. 1, pp. 1-6, 2017.
- [47] S. M. Afonin, “Electroelastic actuator nano- and micro displacement for precision mechanics,” *Am J. Mech. Appl.*, vol. 6, no. 1, pp. 17-22, 2018. <https://doi.org/10.11648/j.ajma.20180601.14>.
- [48] M. Muralidhara, N. J. Vasa, and S. Makaram, “Investigations on a directly coupled piezoactuated tool feed system for micro-electro-discharge machine,” *Int J. Mach. Tool. Manu.*, vol. 49, no. 15, pp. 1197-1203, 2009. <https://doi.org/10.1016/j.ijmachtools.2009.08.004>.
- [49] M. Meraj and S. Pal, “The effect of temperature on creep behaviour of porous (1 at.%) nano crystalline nickel,” *T. Indian I. Metals.*, vol. 69, no. 2, pp. 277-282, 2015. <https://doi.org/10.1007/s12666-015-0763-x>.
- [50] D. Liu and D. J. Pons, “Crack propagation mechanisms for creep fatigue: A consolidated explanation of fundamental behaviors from initiation to failure,” *Metals*, vol. 8, no. 8, pp. 623-623, 2018. <https://doi.org/10.3390/met8080623>.
- [51] B. Merle, “Creep behavior of gold thin films investigated by bulge testing at room and elevated temperature,” *J. Mater. Res.*, vol. 34, pp. 69-77, 2019. <https://doi.org/10.1557/jmr.2018.287>.
- [52] Y. F. Liu, J. J. Shan, U. Gabbert, and N. M. Qi, “Hysteresis and creep modeling and compensation for a piezoelectric actuator using a fractional-order Maxwell resistive capacitor approach,” *Smart Mater. Struct.*, vol. 22, no. 11, Article ID: 115020, 2013. <https://doi.org/10.1088/0964-1726/22/11/115020>.
- [53] W. Hang, X. W. Huang, M. Liu, and Y. Ma, “On the room-temperature creep behavior and its correlation with length scale of a Litao3 single crystal by spherical nanoindentation,” *J. List Mater.*, vol. 12, no. 24, pp. 4213-4213, 2019. <https://doi.org/10.3390/ma12244213>.
- [54] J. D. Bornberger and D. E. Seborg, “Estimation of model order from input-output data applied to radial basis function network identification,” *IFAC Proc. Vol.*, vol. 30, no. 9, pp. 31-36, 1997. [https://doi.org/10.1016/S1474-6670\(17\)43135-1](https://doi.org/10.1016/S1474-6670(17)43135-1).
- [55] C. A. Schmidt, S. I. Bagola, J. E. Cousseau, and J. L. Figueroa, “Volterra-type models for nonlinear systems identification,” *Appl. Math. Model.*, vol. 38, no. 9-10, pp. 2414-2421, 2014. <http://dx.doi.org/10.1016/j.apm.2013.10.041>.
- [56] N. I. Xiros and I. K. Chatjigeorgiou, “Nonlinear identification and input-output representation of the modal dynamics of marine slender structures,” *J. Offshore Mech. Arct. Eng.*, vol. 129, no. 3, pp. 188-200, 2007. <https://doi.org/10.1115/1.2746391>.
- [57] D. Anastasio and S. Marchesiello, “Free-decay nonlinear system identification via mass-change scheme,” *Shock Vib.*, vol. 2019, Article ID: 1759198, 2019. <https://doi.org/10.1155/2019/1759198>.
- [58] V. Prasad, K. Kothari, and U. Mehta, “Parametric identification of nonlinear fractional Hammerstein models,” *Fractal Fract.*, vol. 4, no. 1, pp. 2-2, 2020. <https://doi.org/10.3390/fractalfract4010002>.
- [59] T. S. Pan, T. K. Dao, T. T. Nguyen, and S. C. Chu, “Hybrid particle swarm optimization with bat algorithm,” In *Genetic and Evolutionary Computing*, H. Sun, C. Y. Yang, C. W. Lin, J. S. Pan, V. Snasel, and A. Abraham (Eds.), Springer, Cham., vol. 329, 2015. [https://doi.org/10.1007/978-3-319-12286-1\\_5](https://doi.org/10.1007/978-3-319-12286-1_5).
- [60] H. Garg, “A hybrid PSO-GA algorithm for constrained optimization problems,” *Appl. Math. Comput.*, vol. 274, pp. 292-305, 2016. <https://doi.org/10.1016/j.amc.2015.11.001>.
- [61] J. A. Lazzús, M. Rivera, I. Salfate, G. Pulgar-Villarroel, and P. Rojas, “Application of particle swarm+ant colony optimization to calculate the interaction parameters on phase equilibria,” *J. Eng. Thermophys.*, vol. 25, no. 2, pp. 216-226, 2016. <https://doi.org/10.1134/S1810232816020065>.
- [62] J. Nishtha and B. Suri, “Particle swarm and genetic algorithm applied to mutation testing for test data generation: A comparative evaluation,” *Comput. Inform. Sci.*, vol. 32, no. 4, pp. 514-521, 2020. <https://doi.org/10.1016/j.jksuci.2019.05.004>.

- [63] M. L. Ren, X. D. Huang, X. X. Zhu, and L. J. Shao, "Optimized PSO algorithm based on the simplicial algorithm of fixed point theory," *Appl. Intell.*, vol. 50, pp. 2009-2024, 2020. <https://doi.org/10.1007/s10489-020-01630-6>.
- [64] H. Tran-Ngoc, S. Khatir, G. De Roeck, T. Bui-Tien, L. Nguyen-Ngoc, and M. Abdel Wahab, "Model updating for Nam O bridge using particle swarm optimization algorithm and genetic algorithm," *Sens.*, vol. 18, no. 12, pp. 4131-4131, 2018. <https://doi.org/10.3390/s18124131>.
- [65] Y. J. Gong, J. J. Li, Y. C. Zhou, Y. Li, H. S. H. Chung, Y. H. Shi, and J. Zhang, "Genetic learning particle swarm optimization," *IEEE T. Cybernetics*, vol. 46, no. 10, pp. 2277-2290, 2016. <https://doi.org/10.1109/TCYB.2015.2475174>.
- [66] E. M. Aylward, P. A. Parrilo, and J. J. E. Slotine, "Stability and robustness analysis of nonlinear systems via contraction metrics and SOS programming," *Automatica*, vol. 44, no. 8, pp. 2163-2170, 2007. <https://doi.org/10.1016/j.automatica.2007.12.012>.
- [67] S. Nogueira, K. Sechidis, and G. Brown, "On the stability of feature selection algorithms," *J. Mach. Learn. Res.*, vol. 18, pp. 1-54, 2018.
- [68] J. Berberich, J. Kohler, M. A. Muller, and F. Allgower, "Data-driven model predictive control with stability and robustness guarantees," *IEEE T. Automat. Contr.*, vol. 66, no. 4, pp. 1702-1717, 2021. <https://doi.org/10.1109/TAC.2020.3000182>.
- [69] J. M. Wang, "Explicit solution and stability of linear time-varying differential state space systems," *Int J. Control Autom.*, vol. 15, no. 4, pp. 1553-1560, 2017. <https://doi.org/10.1007/s12555-015-0404-5>.
- [70] S. Safavi and U. A. Khan, "Asymptotic stability of LTV systems with applications to distributed dynamic fusion," *IEEE T. Automat. Contr.*, vol. 62, no. 11, pp. 5888-5893, 2017. <https://doi.org/10.1109/TAC.2017.2648501>.
- [71] B. Bhiri, C. Delattre, M. Zasadzinski, and K. Abderrahim, "Finite-time boundedness and stabilization by a nonlinear state feedback of nonlinear quadratic systems subject to norm-bounded disturbances," *IET Control. Theory A.*, vol. 11, no. 1, pp. 1648-1657, 2017. <https://doi.org/10.1049/iet-cta.2016.1434>.
- [72] F. M. Zaihidee, S. Mekhilef, and M. Mubin, "Robust speed control of PMSM using sliding mode control (SMC)-A review," *Energies*, vol. 12, no. 9, pp. 1669-1669, 2019. <https://doi.org/10.3390/en12091669>.
- [73] S. Kanthalakshmi and W. P. Annal, "Real time implementation of adaptive sliding mode controller for a nonlinear system," *Stud. Inform. Control.*, vol. 27, no. 4, pp. 395-402, 2018. <https://doi.org/10.24846/v27i4y201803>.
- [74] R. Konwar, "A review on sliding mode control: An approach for robust control process," *ADB U J. Electr. Electron. Eng.*, vol. 1, no. 1, pp. 6-13, 2017.
- [75] G. Vighneswaran and K. S. Nair, "Speed control of electric vehicle with sliding mode controller," *Int Res J. Eng. Technol.*, vol. 5, no. 5, pp. 388-391, 2018.
- [76] M. Augustine, "Sliding mode control and chattering: The concept," Project: Sliding Mode Control, vol. 2019, pp. 1-7, 2019. <https://doi.org/10.13140/RG.2.2.35872.23042>.
- [77] A. Ounissi, K. Yakoub, A. Kaddouri, and R. Abdisamad, "Robust adaptive displacement tracking control of piezo-actuated stage," In *2017 6th International Conference on Systems and Control (ICSC)*, Batna, Algeria, May 7-9, 2017, IEEE, pp. 297-302. <https://doi.org/10.1109/ICoSC.2017.7958695>.
- [78] Z. A. Khan, V. Chacko, and H. Nazir, "A review of friction models in interacting joints for durability design," *Friction*, vol. 5, no. 1, pp. 1-22, 2017. <https://doi.org/10.1007/s40544-017-0143-0>.
- [79] A. Ounissi, A. Rachid, and A. Kaddouri, "Robust adaptive backstepping displacement tracking control with application for piezoelectric actuators," *Electromotion*, vol. 17, no. 2, pp. 125-130, 2010.
- [80] R. Coban, "Backstepping integral sliding mode control of an electromechanical system," *Automatik*, vol. 58, no. 3, pp. 266-272, 2018. <https://doi.org/10.1080/00051144.2018.1426263>.
- [81] S. Zhang, E. M. Yong, Y. Zhou, and W. Q. Qian, "Dynamic backstepping control for pure-feedback nonlinear systems," *IMA J. Math. Control. I.*, vol. 37, no. 2, pp. 670-693, 2020. <https://doi.org/10.1093/imamci/dnz019>.